JOC Article

Structural Effects on the Ground and Excited-state Properties of Photoswitchable Hydrogen-Bonding Receptors

Yann Molard,[†] Dario M. Bassani,*[,‡] Jean-Pierre Desvergne,[‡] Nina Moran,[§] and James H. R. Tucker*[,§]

U.M.R. 6226 Sciences Chimiques de Rennes, University Rennes 1, 35042 Rennes, France, LCOO CNRS UMR 5802, University Bordeaux 1, 33405 Talence, France, and School of Chemistry, University of Birmingham, Edgbaston, B15 2TT Birmingham, United Kingdom

d.bassani@lcoo.u-bordeaux1.fr; j.tucker@bham.ac.uk.

Received July 24, 2006

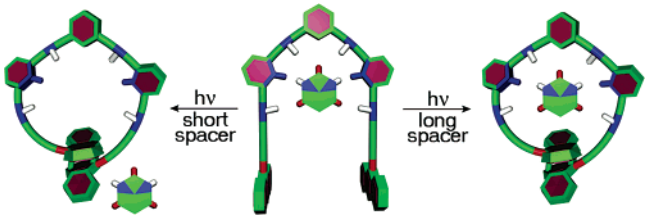

The ground- and excited-state properties of a series of photochromic barbiturate receptors (*N*,*N*′-bis{6-[ω-(anthracen-9-yloxy)alkanoylamino]pyridin-2-yl}-5-*t*-butyl-isophthalamide, **T*n***), in which anthracene chromophores are tethered via $(CH_2)_n$ ($n = 1$, 3−6) polymethylene linkers to the H-bond receptor moiety, are described. In these systems, the thermally reversible [$4\pi + 4\pi$] photodimerization of the anthracenes yields macrocyclic receptors (**T*n*C**) that possess significantly reduced affinity toward barbital as compared to their acyclic counterparts. The length of the tether not only determines the overall binding ability of the cyclized receptor but also has a profound influence on the photochemical and photophysical properties of the anthracene chromophores. The reduced mobility experienced by the covalently bound anthracenes controls the reactivity of a fluorescent excimer that is proposed to be an intermediate in the photocyclization process.

Introduction

There is continuing interest in the development of various methods that enable a response to an external stimulus to control, or be controlled by, a supramolecular binding event.[1] Within this area, switchable binding processes allow for the in situ and noninvasive control of host−guest interactions in a reversible manner and are directly relevant to a number of different and topical research areas, for example, the external control of biological[2] (e.g., DNA−DNA[2a] or DNA−protein[2b]) interactions and controllable molecular motion in interlocked structures.[3]

Of the several types of switchable binding processes that have been explored in host−guest systems in the past,[4,5] photoswitched binding is perhaps the most established.[6,7] As demonstrated in the early examples developed by Shinkai[6a] and Ueno,[7a] such systems can be designed by connecting a photochromic group to a supramolecular receptor. Photoswitched binding (a form of gated photochromism[8]) then results if a light-triggered structural change to the photochromic unit leads to a

* Corresponding authors. (D.M.B.) Tel: +33 540 002 827 and fax: +33 540 006 158. (J.H.R.T.) Tel: +44 121 414 4422 and fax: +44 121 414 4403.
[†] University Rennes 1.
[‡] University Bordeaux 1.
[§] University of Birmingham.

(1) (a) Lehn, J.-M. *Supramolecular Chemistry, Concepts and Perspectives*; VCH: Weinheim, 1995. (b) Petitjean, A.; Kyritsakas, N.; Lehn, J.-M. *Chem.−Eur. J.* **2005**, *11*, 6818 and references therein. (c) For a review of switchable binding processes at a surface, see: Cooke, G. *Angew. Chem., Int. Ed.* **2003**, *42*, 4860.

(2) (a) Asanuma, H.; Takarada, T.; Yoshida, T.; Tamaru, D.; Liang, X. G.; Komiyama, M. *Angew. Chem., Int. Ed.* **2001**, *40*, 2671. (b) Woolley, G. A.; Jaikaran, A. S. I.; Berezovski, M.; Calarco, J. P.; Krylov, S. N.; Smart, O. S.; Kumita, J. R. *Biochemistry* **2006**, *45*, 6075 and references therein. (c) Volgraf, M.; Gorostiza, P.; Numano, R.; Kramer, R. H.; Isacoff, E. Y.; Trauner, D. *Nat. Chem. Biol.* **2006**, *2*, 47 and references therein.

(3) For a recent review of switchable processes in rotaxanes, see: Tian, H.; Wang, Q. C. *Chem. Soc. Rev.* **2006**, *35*, 361.

(4) For recent examples of substrate-switched (e.g., allosteric) binding, see: (a) Abe, H.; Masuda, N.; Waki, M.; Inouye, M. *J. Am. Chem. Soc.* **2005**, *127*, 16189 and references therein. (b) Amendola, V.; Esteban-Gomez, D.; Fabbrizzi, L.; Licchelli, M.; Monzani, E.; Sancenon, F. *Inorg. Chem.* **2005**, *44*, 8690.

(5) For examples and reviews of redox-switched binding processes, see: (a) Bu, J. J.; Lilienthal, N. D.; Woods, J. E.; Nohrden, C. E.; Hoang, K. T.; Truong, D.; Smith, D. K. *J. Am. Chem. Soc.* **2005**, *127*, 6423 and references therein. (b) Tucker, J. H. R.; Collinson, S. R. *Chem. Soc. Rev.* **2002**, *31*, 147.

10.1021/jo061528a CCC: $33.50
Published on Web 09/30/2006

reversible change in guest binding affinity. Most examples of photoswitched binding in the literature have involved metal cation binding systems,[6] where a photochromic unit (e.g., azobenzene) is attached to a suitable binding unit such as a crown ether. It is somewhat surprising that the photoswitched binding of species other than metal cations, for example, those bound through H-bonding interactions, has been studied in less detail.[7,9]

Over the past few years, we[10] and others[11] have studied anthracene photochromism, which operates through a thermally reversible [4π + 4π] photodimerization reaction, and its use in photoswitched metal cation binding by anthracene-based receptors. Here, we report our studies on a series of photoswitchable receptors, **T*n***, that display marked photoswitched binding behavior toward H-bonding neutral molecules as a result of anthracene photodimerization (Scheme 1). The well-established barbital receptor system developed by Hamilton[12,13] was selected as a potential binding motif, whose strong affinity for the substrate could be modulated by conversion between an acyclic and a macrocyclic form. Very promising preliminary results, obtained with a trimethylene linker (**T3**),[14] encouraged us to investigate the influence of the size of the macrocyclic cavity. By varying the length of the tethers connecting the anthracene moieties to the receptor unit, variously sized macrocycles were

SCHEME 1

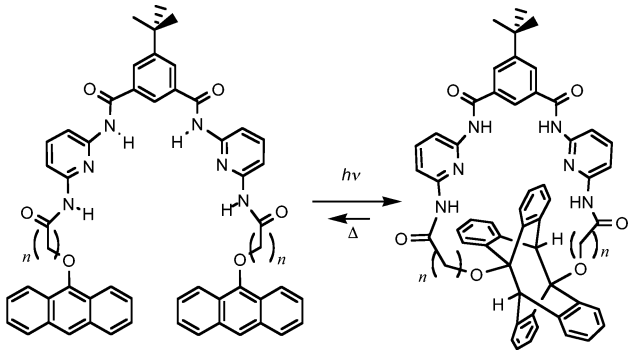

obtained upon photocyclization. The results obtained illustrate the delicate balance between conformational control of excimer reactivity and host−guest interactions and how this affects the photochemical and photophysical properties of the acyclic receptors.

Results

Synthesis. Scheme 2 illustrates the route taken for the synthesis of the bis-anthracene receptors **T*n*** (*n* = 1, 3, 4, 5, 6). Starting from commercially available anthrone **1**, the corresponding carboxylic acid derivatives **3*n*** were prepared via alkylation with ethyl-*n*-bromoalkanoate (K_2CO_3, acetone) followed by hydrolysis of the ester group (aqueous NaOH, ethanol). In the case of ethyl 2-bromopropanoate, elimination of HBr proved faster than nucleophilic substitution, and the desired carboxylic acid **3₂** could not be obtained. Coupling between **3*n*** and 2,6-diaminopyridine were performed in two steps via the corresponding *N*-succinimidoyl ester intermediate (**4*n***, prepared by reaction with *N*-hydroxysuccinimide and *N*,*N*′-dicyclohexylcarbodiimide in ethyl acetate at 25 °C) by reaction with an excess of 2,6-diaminopyridine in dry CH_2Cl_2 and diisopropylethylamine (1.5 mol. equiv). The acyclic receptors **T*n*** were obtained in good yield (60−75%) by amide bond formation between the acyl chloride of the 5-tertbutyl isophthalic acid and the **5*n*** compounds in THF in the presence of triethylamine followed by purification by column chromatography on alumina (CH_2Cl_2/MeOH gradient).

Irradiation Studies. The conversion of receptors **T*n*** to their respective photoproducts **T*n*C** (*n* = 3, 4, 5, 6) (Scheme 1) was achieved by irradiating a CH_2Cl_2 solution of the receptor with a high-pressure Hg lamp at λ > 330 nm (lead nitrate/sodium bromide filter, 7 g L^{-1}/KBr 540 g L^{-1}).[15] High dilution

(6) For examples and reviews of photoswitched binding of metal cations, see: (a) Shinkai, S.; Nakaji, T.; Nishida, Y.; Ogawa, T.; Manabe, O. *J. Am. Chem. Soc*. **1980**, *102*, 5860. (b) Kimura, K.; Sakamoto, H.; Nakamura, M. *Bull. Chem. Soc. Jpn*. **2003**, *76*, 225. (c) Alfimov, M. V.; Fedorova, O. A.; Gromov, S. P. *J. Photochem. Photobiol., A* **2003**, *158*, 183. (d) Bacchi, A.; Carcelli, M.; Pelizzi, C.; Pelizzi, G.; Pelagatti, P.; Rogolino, D.; Tegoni, M.; Viappiani, C. *Inorg. Chem*. **2003**, *42*, 5871. (e) Desvergne, J.-P.; Bouas-Laurent, H.; Perez-Inestrosa, E.; Marsau, P.; Cotrait, M. *Coord. Chem. Rev*. **1999**, *185*−*186*, 257 and references therein.

(7) For photoswitched binding of charged or neutral molecules, see: (a) Ueno, A.; Yoshimura, H.; Saka, R.; Osa, T. *J. Am. Chem. Soc*. **1979**, *101*, 2779. (b) Mulder, A.; Jukovic, A.; Huskens, J.; Reinhoudt, D. N. *Org. Biomol. Chem*. **2004**, *2*, 1748 and references therein; (c) Hunter, C. A.; Togrul, M.; Tomas, S. *Chem. Commun*. **2004**, 108. (d) Goodman, A.; Breinlinger, E.; Ober, M.; Rotello, V. M. *J. Am. Chem. Soc*. **2001**, *123*, 6213.

(8) Bouas-Laurent, H.; Dürr, H. *Pure Appl. Chem*. **2001**, *73*, 639.

(9) For examples and reviews of related H-bonding photoresponsive systems, see: (a) Huang, C. H.; Bassani D. M. *Eur. J. Org. Chem*. **2005**, 4041. (b) Yagai, S.; Karatsu, T.; Kitamura, A. *Chem.*−*Eur. J*. **2005**, *11*, 4054. (c) Vida Pol, Y.; Suau, R.; Perez-Inestrosa, E.; Bassani, D. M. *Chem. Commun*. **2004**, 1270 and references therein. (d) Lucas, L. N.; van Esch, J.; Kellogg, R. M.; Feringa, B. L. *Chem. Commun*. **2001**, 759. (e) Vollmer, M. S.; Clark, T. D.; Steinem, C.; Ghadiri, M. R. *Angew. Chem., Int. Ed*. **1999**, *38*, 1598. (f) Würther, F.; Rebek, J., Jr. *Angew. Chem., Int. Ed. Engl*. **1995**, *34*, 446. (g) Irie, M.; Miyatake, O.; Uchida, K.; Eriguchi, T. *J. Am. Chem. Soc*. **1994**, *116*, 9894. (h) Bassani, D. M.; Sallenave, X.; Darcos, V.; Desvergne, J.-P. *Chem. Commun*. **2001**, 1446.

(10) (a) Bouas-Laurent, H.; Castellan, A.; Desvergne, J.-P.; Lapouyade, R. *Chem. Soc. Rev*. **2000**, *29*, 43. (b) Bouas-Laurent, H.; Castellan, A.; Desvergne, J.-P.; Lapouyade, R. *Chem. Soc. Rev*. **2001**, *30*, 248. (c) McSkimming, G.; Tucker, J. H. R.; Bouas-Laurent, H.; Desvergne, J.-P.; Coles, S. J.; Hursthouse, M. B.; Light, M. E. *Chem.*−*Eur. J*. **2002**, *8*, 3331 and references therein. (d) Desvergne, J.-P.; Bitit, N.; Castellan, A.; Bouas-Laurent, H.; Soulignac, J.-C. *J. Lumin*. **1987**, *37*, 175. (e) Ferguson, J.; Castellan, A.; Desvergne, J.-P.; Bouas-Laurent, H. *Chem. Phys. Lett*. **1981**, *78*, 446 and references therein. (f) Marquis, D.; Desvergne, J.-P. *Chem. Phys. Lett*. **1994**, *230*, 131.

(11) For other examples of photoswitched cation binding via anthracene photodimerization, see: (a) Schafer, C.; Mattay, J. *Photochem. Photobiol. Sci*. **2004**, *3*, 331. (b) Ikegami, M.; Ohshiro, I.; Arai, T. *Chem. Commun*. **2003**, 1566. (c) Deng, G.; Sakaki, T.; Nakashima, K.; Shinkai, S. *Chem. Lett*. **1992**, 1287. For examples of photoswitched cation transport via anthracene photodimerization, see: (a) Xu, M.; Fu, X. G.; Wu, L. Z.; Zhang, L. P.; Tung, C. H. *Phys. Chem. Chem. Phys*. **2002**, *4*, 4030. (d) Jin, T. *Chem. Commun*. **2000**, 1379.

(12) (a) Chang, S.-K.; Hamilton, A. D. *J. Am. Chem. Soc*. **1988**, *110*, 1318. (b) Chang, S.-K.; Van Engen, D.; Fan, E.; Hamilton, A. D. *J. Am. Chem. Soc*. **1991**, *113*, 7640.

(13) For examples of supramolecular assemblies based on barbiturate−receptor interactions, see: (a) Lipkowski, P.; Bielejewska, A.; Timmerman, P.; Reinhoudt, D. N.; Kooijman, H.; Spek, A. L. *Chem. Commun*. **1999**, 1311. (b) Prins, L. J.; Reinhoudt, D. N.; Timmerman, P. *Angew. Chem., Int. Ed*. **2001**, *40*, 2382. (c) Russell, K. C.; Lehn, J. M.; Kyritsakas, N.; DeCian, A.; Fischer, J. *New J. Chem*. **1998**, *22*, 123. (d) Berl, V.; Schmutz, M.; Krische, M. J.; Khoury, R. G.; Lehn, J.-M. *Chem.*−*Eur. J*. **2002**, *8*, 1227. (e) Kolomiets, E.; Lehn, J.-M. *Chem. Commun*. **2005**, 1519. (f) Kolomiets, E.; Buhler, E.; Candau, S. J.; Lehn, J. M. *Macromolecules* **2006**, *39*, 1173. (g) Dirksen, A.; Hahn, U.; Schwanke, F.; Nieger, M.; Reek, J. N. H.; Voegtle, F.; De Cola, L. *Chem.*−*Eur. J*. **2004**, *10*, 2036. (h) Dirksen, A.; Kleverlaan, C. J.; Reek, J. N. H.; De Cola, L. *J. Phys. Chem. A* **2005**, *109*, 5248. (i) McClenaghan, N. D.; Grote, Z.; Darriet, K.; Zimine, M.; Williams, R. M.; De Cola, L.; Bassani, D. M. *Org. Lett*. **2005**, *7*, 807. (j) Schmittel, M.; Kalsani, V. *Top. Curr. Chem*. **2005**, *245*, 1.

(14) Molard, Y.; Bassani, D. M.; Desvergne, J.-P.; Horton, P. N.; Hursthouse, M. B.; Tucker, J. H. R. *Angew. Chem., Int. Ed*. **2005**, *44*, 1072.

(15) Schönberg, A. *Preparative Organic Photochemistry*; Springer-Verlag: Berlin, 1968; p 492.

SCHEME 2[a]

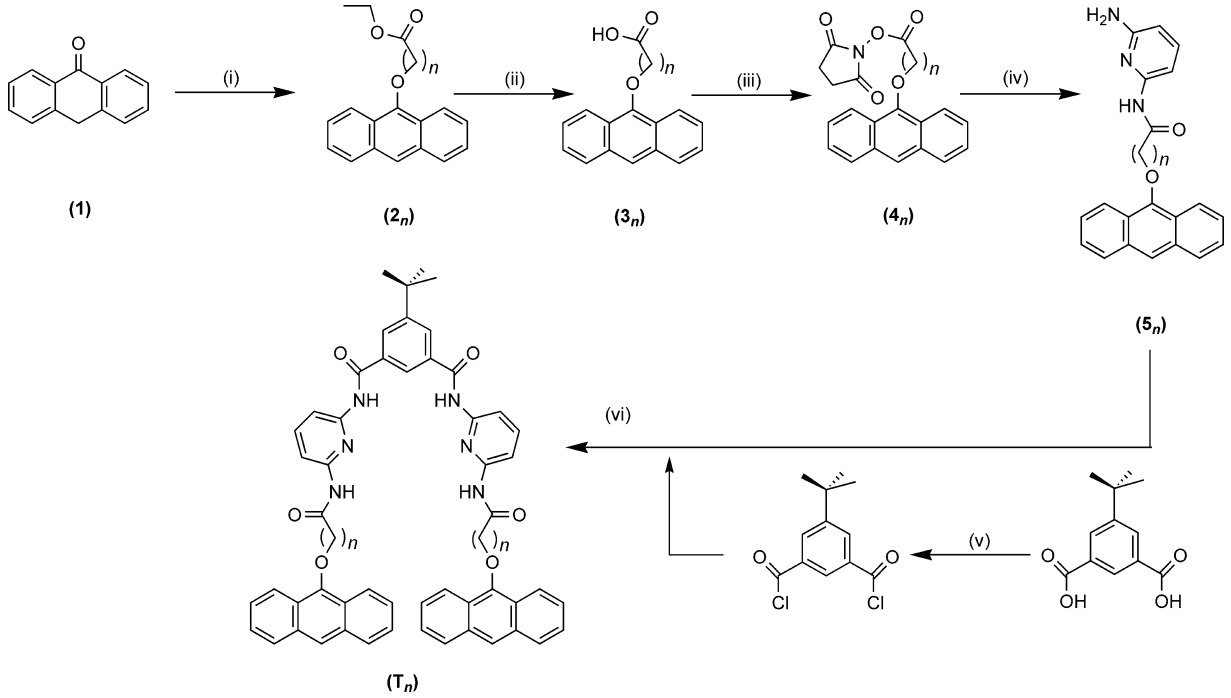

[a] Reagents: (i) $Br(CH_2)_nCO_2Et$, K_2CO_3, acetone, reflux, 14 h; (ii) 1) $NaOH_{aq}$, EtOH, reflux, 14 h; 2) H_2O, HCl; (iii) NHS, DCC, ethyl acetate, 25 °C, 48 h; (iv) 2,6-diaminopyridine, DIEA, CH_2Cl_2, reflux, 5 days; (v) oxalyl chloride, CH_2Cl_2, reflux, 14 h; and (vi) triethylamine, THF, 25 °C, 14 h.

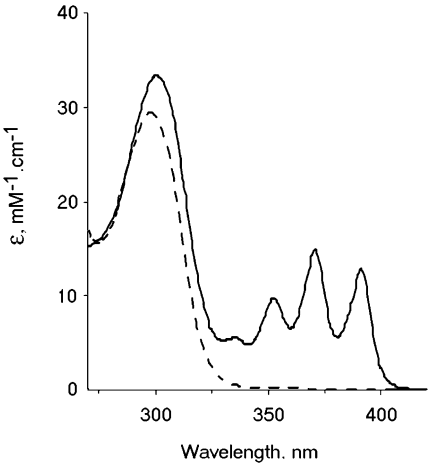

FIGURE 1. Absorption spectra of **T4** and **T4C** in CH_2Cl_2. The spectra of the other **T*n*** and **T*n*C** compounds are similar (data not shown).

conditions ($\leq 5 \times 10^{-4}$ M) and degassed solvents were used to avoid intermolecular processes and oxidation of the anthracene moieties. The reaction was followed by UV−vis spectroscopy by monitoring the disappearance of the long-wavelength anthracene absorption band (350−420 nm). Once the reactions had gone to completion, evaporation of the solutions gave the products as white solids in quantitative yield. The UV−vis absorption spectra of **T4** and **T4C** measured in CH_2Cl_2 are representative (Figure 1). The spectra of the remaining acyclic and macrocyclic forms of the receptors are very similar (data not shown). All compounds possess a band centered at approximately 300 nm, due to absorption by pyridine units, while the acyclic forms display the characteristic shape of the first absorption band of anthracene (mainly ^{1}La in character) between 350 and 420 nm. In the case of **T1**, photoirradiation resulted in an uncharacterized mixture of products.

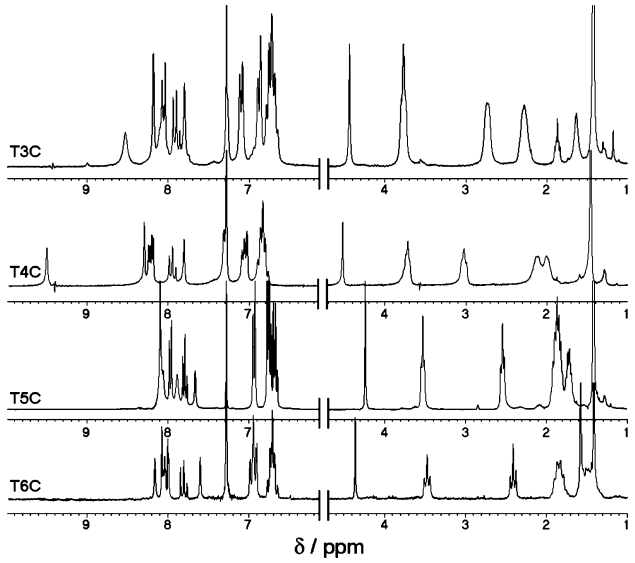

FIGURE 2. ^{1}H NMR spectra of photoproducts **T*n*C** in $CDCl_3$.

Photoproduct Characterization by NMR. The ^{1}H NMR spectra of the isolated photoproducts are shown in Figure 2. The appearance of a new singlet resonance at 4.43, 4.51, 4.24, and 4.36 ppm for **T3C**, **T4C**, **T5C**, and **T6C**, respectively, attributed to the two equivalent bridgehead protons on the photodimer subunit, confirms the occurrence of $[4\pi + 4\pi]$ photocycloaddition between the central rings on each anthracene unit.[10]

The ^{13}C NMR spectra of each photodimer confirmed the symmetrical nature of the products: the signals at 89.9, 90.9, 89.1, and 89.4 ppm for **T3C**, **T4C**, **T5C**, and **T6C**, respectively, correspond to the two new quaternary carbons, whereas those at 63.5, 65.2, 63.8, and 64.0 ppm are assigned to the two sp^3 hybridized CH groups on the central ring.

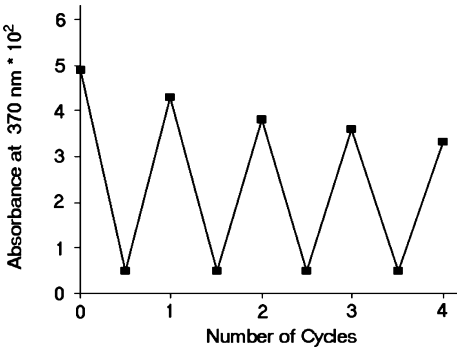

FIGURE 3. Absorbance of the anthracene chromophore in **T5** (ca. 4 × 10^{-6} M, monitored at 370 nm) upon repeated cycling through photoinduced dimerization and thermal retrodimerization (80 °C, 8 h) in degassed toluene.

Fatigue Studies. To examine the ability of the anthracene photochromic system to withstand repeated cycling, degassed toluene solutions of each acyclic receptor were successively irradiated to form the corresponding macrocycle and then immediately heated to regenerate the open form. To complete thermal retrodimerization over a time scale of 24 h, it was necessary to heat the solutions to 80 °C. The concentration of the acyclic form after each opening process was determined by examining the absorption intensity of the ^{1}La band at 370 nm. Although >90% of the acyclic form of each receptor was recovered after each cycle, repetitive cycling leads to slow decomposition, as shown in Figure 3 for **T5** and **T5C**, where the fatigue was 30% after four cycles.[16]

Binding Studies. For comparison purposes, the binding properties of the receptors were focused on two neutral molecules as guest species: barbital **6**, which contains six H-bonding sites and is fully complementary to the receptor site, and the cyclic urea **7**, which has four H-bonding sites.

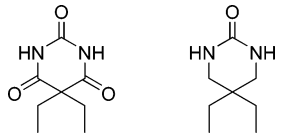

Binding was followed spectroscopically using ^{1}H NMR, UV−vis absorption, and fluorescence spectroscopy. ^{1}H NMR was used when the binding constant was low enough to obtain an accurate value at NMR concentrations ($K \leq 1000$ M^{-1}). UV−vis and fluorescence data were analyzed using the nonlinear regression program LETAGROP,[17] whereas the NMR data were analyzed by EQNMR.[18] The resulting binding constants with **6** and **7** are displayed in Table 1. To confirm the stoichiometry of the complexes, Job plot experiments were performed by UV−vis spectroscopy on **T5** and barbital and by ^{1}H NMR spectroscopy on **T5C** and barbital (Figure S1, Supporting Information). The curves showed a maximum when the molar fraction ratio reached 0.5, consistent with the formation of a 1:1 complex, as illustrated in Figure 4.

TABLE 1. Binding Constant Values, K_{ass} (M^{-1}), at 293 K Obtained for Acyclic (T*n*) and Macrocyclic (T*n*C) Receptors with Barbital, 6, and DPU, 7[a]

	barbital, **6**	DPU, **7**[b]
T3	38000[c]	120
T3C	38[b]	5.6
T4	33000[c]	160
T4C	450[b]	10
T5	62000[c]	76
T5C	8300[d]	8
T6	71000[d]	53
T6C	26000[d]	21

[a] Accuracy within ±15%. [b] In $CDCl_3$ at ca. 3.5 × 10^{-3} M by NMR spectroscopy. [c] In CH_2Cl_2 at ca. 2 × 10^{-6} M by fluorescence spectroscopy. [d] In CH_2Cl_2 at ca. 2.5 × 10^{-5} M by UV−vis spectroscopy.

The ^{1}H NMR spectra of **T*n*** and **T*n*C** ($n = 3$ or 6) in $CDCl_3$ before and after the addition of 1 equiv of barbital are shown in Figure S2 (Supporting Information). With the exception of **T3C**, where binding was very weak, a strong H-bonding interaction was found, as evidenced by the large downfield shift of the two amide signals of each receptor (e.g., +1.47 and +1.58 ppm for **T3**; +1.31 and +1.84 ppm for **T6**; and +1.21 and +1.44 ppm for **T6C**).[19]

The only observable change to the UV−vis spectra of the receptors upon the addition of excess barbital was a bathochromic and slightly hypochromic shift in the pyridine band at 300 nm (Figure 5a), which is associated to an H-bonding interaction involving this group. These changes were used to evaluate binding constants. Emission spectra of the acyclic ligands were obtained in CH_2Cl_2 at low concentrations (ca. 5 × 10^{-6} M) (excitation at 360 nm) and exhibited a structured band with a maximum of intensity at 420 nm assigned to the locally excited species referred to as monomer (Figure 5b). The addition of

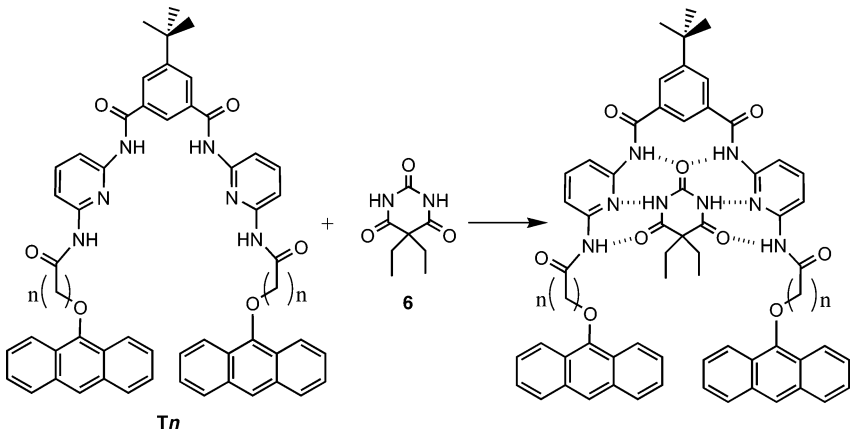

FIGURE 4. Association of **6** and **T*n*** receptors leads to the formation of 1:1 complexes in which **6** is held within the receptor site by six-point H-bonding.

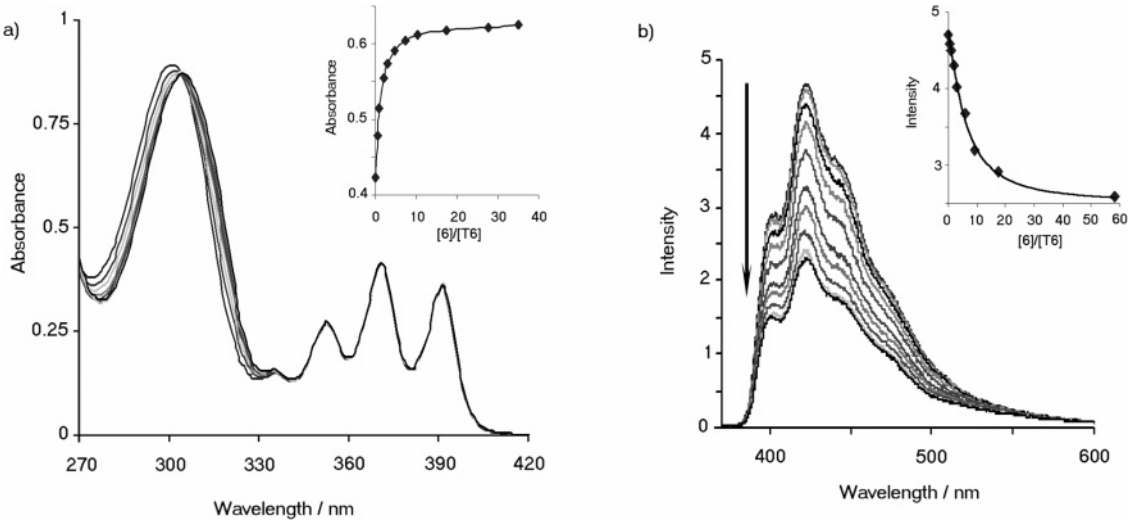

FIGURE 5. (a) Binding of barbital **6** by receptor **T6** as followed by UV−vis spectroscopy in CH_2Cl_2 (concentration = 2.6×10^{-5} M). The inset shows the increase in the observed molar absorption coefficient at 315 nm upon addition of compound **6**. (b) The binding of **6** by receptor **T6** in CH_2Cl_2 as followed by fluorescence spectroscopy. From top down: **T6** at 3.7×10^{-6} M; + 0.5 equiv of **6**; + 1 equiv of **6**; + 2 equiv of **6**; + 3 equiv of **6**; + 6 equiv of **6**; + 9 equiv of **6**; + 17 equiv of **6**; + 60 equiv of **6**; + 120 equiv of **6**; and + 230 equiv of **6**. The inset shows the decrease in fluorescence emission intensity at 420 nm upon addition of compound **6**.

TABLE 2. Kinetic Parameters ($1/\lambda_i$) Obtained from Fluorescence Emission Decay of Receptors T*n* in the Absence and in the Presence of 6[a]

	A_1	$1/\lambda_1$ (ns)	A_2	$1/\lambda_2$ (ns)	χ^2
T1	0.89	3.9	0.08	9.6	0.98
T1:6	0.71	2.6	0.33	6.0	1.09
T3		4.3			1.19
T3:6	0.73	1.9	0.45	8.3	1.03
T4		4.8			1.04
T4:6	0.99	2.4	0.06	9.7	1.03
T5		4.9			1.01
T5:6	1.33	2.2	0.04	8.3	1.07
T6		5.7			1.15
T6:6	0.98	2.2	0.06	4.1	1.16

[a] 20 °C in degassed CH_2Cl_2 at λ_{obs} = 420 nm. Accuracy ±10%.

barbital resulted in a decrease in its fluorescence intensity, which was used to determine binding constants.

Fluorescence Lifetimes and Laser-Induced Fluorescence Experiments. Fluorescence decay profiles were obtained in the absence or in the presence of a large excess of **6** (ca. 1000 equiv) in dichloromethane solutions that were degassed by three freeze−pump−thaw cycles. The data, collected in Table 2, were fitted to a one- or two-exponential decay and the goodness-of-fit judged by the χ^2 values (0.98−1.19) and the residual distribution.

Time-resolved laser-induced fluorescence emission was collected upon the excitation of degassed dichloromethane solutions of **T*n*** (ca. 5×10^{-6} M) in the absence and in the presence of an excess amount of **6** (ca. 1000 equiv) using a frequency tripled Nd:YAG laser (λ = 355 nm, pulse width = 7 ns). The emission was collected at a right angle to the excitation beam and focused on a spectrograph equipped with an ICCD camera. The fluorescence emission after ca. 100 ns delay was corrected for the response curve of the spectrograph and is shown in Figure 6.

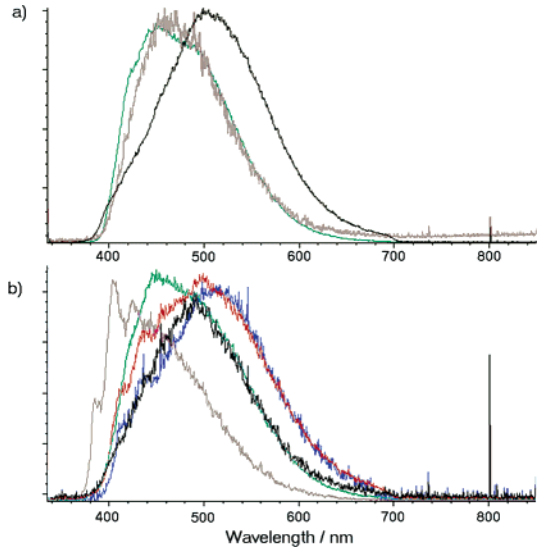

FIGURE 6. Time-resolved laser-induced fluorescence emission spectra (corrected) of receptors **T*n*** (ca. 5×10^{-6} M in degassed CH_2Cl_2) obtained ca. 100 ns after excitation. In the absence (a) and in the presence (b) of a large excess of **6** (ca. 5×10^{-3} M). Green: **T1**; gray: **T3**; black: **T4**; red: **T5**; and blue: **T6**.

Fluorescence and Photodimerization Quantum Yields. The fluorescence and reaction quantum yields were determined in degassed dichloromethane solution according to a previously described methodology.[20] Quinine sulfate in 1 N sulfuric acid

(16) No significant changes in the percentage fatigue were found from cycling in the presence of an excess amount of barbital.

(17) (a) Sillen, L. G.; Warnqvist, B. *Ark. Kemi* **1968**, *31*, 377. (b) Sillen, L. G.; Warnqvist, B. *Ark. Kemi* **1968**, *31*, 315. (b) Havel, J. *Haltafal-Spefo program*; Mazaryle University: Brno, Moravia, Czech Republic.

(18) Hynes, M. J. *J. Chem. Soc., Dalton Trans.* **1993**, 311.

(19) The H-bonded amide proton at 9.5 ppm in **T4C** underwent an upfield shift of 0.15 ppm upon the addition of 5 equiv of barbital to indicate a disruption of the intermolecular H-bonding interactions. Complexation of barbital also affected the signal for the isophthaloyl proton of each receptor, which moved downfield due to its proximity to the apical CO of guest (e.g., +0.2, +0.1, and +0.16 ppm, respectively, for **T3**, **T3C**, and **T6C**).

(20) (a) Melhuish, W. H. *J. Phys. Chem.* **1961**, *65*, 229. (b) Eaton, D. E. In *Handbook of Organic Photochemistry*, Vol. I; Scaiano, J. C., Ed.; CRC: Boca Raton, FL, 1989.

TABLE 3. Fluorescence Quantum Yield (Φf) and Intramolecular Photocycloaddition Quantum Yield (Φr) in the Absence and in the Presence of an Excess of 6 at Room Temperature[a]

	Φf		Φr	
	T*n*	**T*n*:6**	**T*n***	**T*n*:6**
T1	0.29	0.24		
T3	0.34	0.25	0.07	0.01
T4	0.23	0.15	0.15	0.05
T5	0.30	0.20	0.07	0.05
T6	0.21	0.10	0.09	0.16

[a] Accuracy ±15%.

was used as a secondary standard for fluorescence emission intensity upon excitation at 366 nm ($\Phi_f = 0.54$). Photoreaction quantum yields were determined upon excitation at 366 nm using Aberchrome 540 as a chemical actinometer on an optical bench equipped with a 2000 W Hg−Xe lamp and a monochromator. Samples (5×10^{-5} M) were stirred during the irradiation, and the amount of converted material was determined at 10 min intervals by UV−vis spectroscopy using the disappearance of the ^{1}La band of the anthracene moieties at 370 nm until 90% of the starting material was converted. No spontaneous recovery of the anthracene absorption band was observed upon resting the irradiated samples at room temperature. The results are collected in Table 3.

Discussion

The compounds **T*n*** are designed to bind **6** and **7** through multiple-point H-bonding interactions. The binding sites are not conjugated to the anthracene chromophore, and it is therefore not surprising that only minor effects are observed in the electronic absorption spectra of **T*n*** upon binding of **6** or **7** (Figure 5a). In contrast, a significant quenching of the fluorescence emission of the anthracene moiety is observed upon complexation of **6** (Figure 5b), indicative of more important effects on the excited-state potential energy surface. The decrease of the fluorescence presumably results from conformational changes in the receptor moiety, which brings the two anthracene subunits closer. Whereas this would be expected to favor photodimerization or intramolecular self-quenching, no concomitant increase in Φr is observed for receptors up to and including **T5** (Table 3). A plausible explanation is that the binding of **6** favors the formation of a weakly emissive excimer that is either not involved in the photodimerization reaction or, more likely, whose dimerization is also chain-length dependent. In support of this, close inspection of the steady-state fluorescence emission spectra presented in Figure 5b reveals a slight increase in emission at longer wavelengths, a feature sometimes observed in cases where a weakly fluorescent excimer is present. To further investigate this point, time-resolved laser induced fluorescence (LIF) was used to detect the presence of excimer emission at longer lifetimes. In the absence of **6**, the results clearly show the presence of broad, long-wavelength emission with very low intensity only for $n = 1$, 3, and 4 with an emission maximum located at ca. 470, 465, and 505 nm, respectively (Figure 6a). In contrast, the addition of barbital induces stronger excimer emission for all the acyclic receptors except $n = 1$ with maxima at 465, 495, 505, and 510 nm for $n = 3$, 4, 5, and 6, respectively (Figure 6b). The structural features that are observed in the excimer emission are attributed to emission arising from the locally excited chromophores.[21] The increase in the wavelength maximum presumably reflects a more extended overlap of the two anthracene moieties as a function of increasing spacer length.

The observation of a second decay component in the excited singlet-state lifetimes presented in Table 2 corroborates the existence of an emissive excimer for the **T*n*** receptors in the presence of barbital **6**. In analogy with previously investigated intramolecular excimer-forming systems,[10b] the shorter decay parameter (1.9−2.2 ns) is attributed to the emission of the locally excited anthracene chromophore (monomer). The longer decay component, which is accordingly attributed to excimer emission, first increases with increasing chain length (**T1**, **T3**, and **T4**), then decreases as the tether is further lengthened (**T4**, **T5**, and **T6**). The optimum chain length for stabilizing the excimer is expected to be a tradeoff between entropic contributions in bringing the two chromophores in contact within the excited-state lifetime of the locally excited-state and enthalpic contributions due to conformational strain in the shorter polymethylene chains. As noted previously, excimer emission in the absence of **6** is extremely weak, and the observed emission decay in this case can be adequately fitted by a monoexponential decay. With the exception of **T1**,[22] the fluorescence lifetimes (4.3−5.7 ns) thus reflect the decay of the locally excited anthracene chromophores and are typical of 9-substituted anthracenes.[10]

The data obtained from spectroscopic investigations were combined and used to determine binding constants with guests **6** and **7**, as presented in Table 1. In the case of **T5** and **T6**, the binding constant with barbital was investigated by both UV−vis and fluorescence spectroscopy ($K_{ass} = 2.5 \times 10^4$ and 6.2×10^4 M^{-1} for **T5** and $K_{ass} = 7.1 \times 10^4$ and 4.4×10^4 M^{-1} for **T6**, as determined from absorption and fluorescence data, respectively). Differences between binding constants determined by these two techniques have previously been observed and ascribed to conformational changes in the receptor during the excited-state lifetime of chromophore.[10f] It is immediately obvious from the data in Table 1 that photocyclization of the terminal anthracene moieties has a profound effect on the host−guest interactions of these compounds. In the case of **6**, binding to the acyclic receptors **T*n*** is very strong, and the observed association constants vary little with chain length. This contrasts markedly with the cyclized receptors **T*n*C**, for whom the association constants are very low and increase substantially with increasing chain length. The lower affinities observed for the macrocyclic receptors as compared to their acyclic counterparts (i.e., $\log(K_{ac}/K_c) > 0$, Figure 7) contrast with previous results for cyclic versus acyclic systems reported by Hamilton in which much higher binding affinities for structurally confined macrocyclic receptors were observed as compared to their acyclic counterparts.[12]

This switch in behavior can be explained by examining the solid-state crystal structures of the cyclized receptors **T3C** and **T5C** (Figure 8).[14] Photodimerization of the anthracene chromophores results in the formation of HT dimers whose steric bulk partly blocks the H-bonding cavity of the receptor moiety. This effect is much more important in **T3C** due to the shorter length of the polymethylene tether. As a result, this effectively

(21) It is also possible that the excimer is in equilibrium with the locally excited-state.

(22) The reduced spacer length in **T1** is expected to limit the mobility of the chromophores due to restricted conformational freedom of the amide linker. The ensuing biexponential decay may be due to the presence of excimer fluorescence or kinetically distinct nonequilibrating locally excited-states.

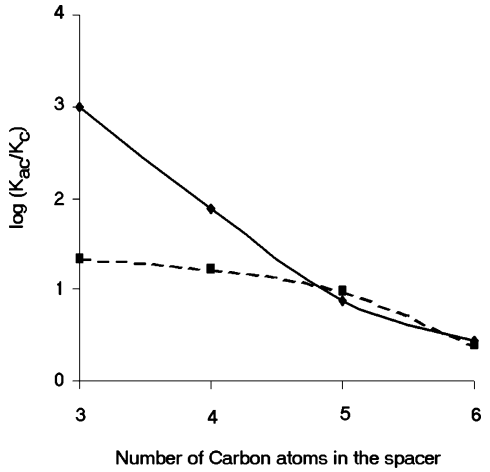

FIGURE 7. Ratio of binding affinities for the open and closed form of the receptor as a function of spacer length for compound **6** (plain line) and compound **7** (dashed line).

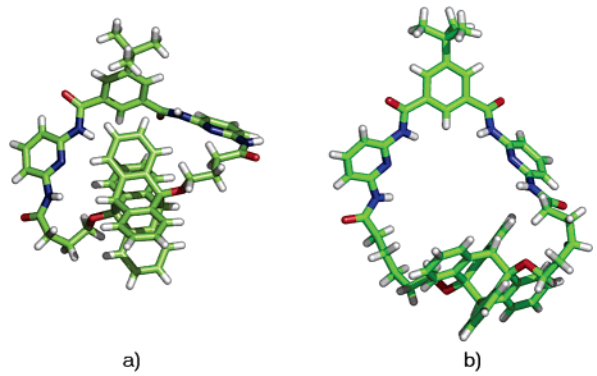

FIGURE 8. X-ray structures of **T3C** and **T5C**.[14]

prohibits simultaneous binding of the guest to both arms of the receptor, and the observed binding constants are typical of three-point H-bonding observed in analogous A−D−A systems.[23] However, in the case of the larger macrocycles **T5C** and **T6C**, the high binding constants indicate that the longer chains allow simultaneous binding of the guest to both arms within the cavity but in a suprafacial mode, facilitated by the flexibility of the penta- or hexa-methylene chains in solution. The large upfield shift in the CH_3 resonance of the barbital ethyl group upon complexation with **T5C** and **T6C** (−0.54 and −0.68 ppm as compared to the complexes of **6** with their respective acyclic forms) is indicative of the proximity of the cavity-bound guest to the aromatic xylene units,[24] as found by Hamilton for complexes of **6** with related naphthyl macrocycles.[12]

The association constants between DPU, **7**, and the receptors in their acyclic and cyclic forms are also displayed in Table 3. As expected, the binding constants are much smaller than those with **6** due to the formation of only four H-bonds with the guest, as evidenced by the fact that only the resonance of the two amide protons nearest the isophthaloyl unit undergoes a significant downfield shift upon complexation (see Supporting Information). This information suggests that **7** is inserted within the cavity of each acyclic receptor in a fashion similar to **6**, with the formation of two H-bonds from the isophthalyl amide N−H groups to the C2 carbonyl in **7**. The higher binding affinities toward **7** displayed by the receptors with shorter linkers (**T3** and **T4**) is interesting and may be related to the proximity of the two anthracene chromophores. The ensuing hydrophobic cavity would enhance binding, and its effect would be expected to decrease with increasing chain length, as is observed. Here too, binding constants decrease substantially upon photocyclization of the receptor, although not as dramatically as in the case of **6**, which results in a less steep curve for **7** as depicted in Figure 7 (dashed line).

Straightforward interpretation of the association constants presented in Table 1 is, at least in some cases, rendered difficult by the occurrence of intramolecular H-bonding between the two arms of the receptor moiety. This is certainly the case for **T4C**, where the unusual downfield shift of the broad singlet ascribed to the two amide protons closest to the anthracenes[25] indicates the existence of an intramolecular H-bond (Figure 2, confirmed as intramolecular by dilution experiments). In this compound, it is likely that the hydrogen-bond acceptor is the oxygen atom adjacent to the anthracene photodimer since the signal for the photodimer bridgehead proton (at 4.51 ppm) is further downfield than for the other macrocycles. This is also reflected in the ^{13}C signal for the adjacent methylene group, which resonates at 67.8 ppm (as compared to 63.5, 64.5, and 64.7 ppm for **T3C**, **T5C**, and **T6C**, respectively).

The photoinduced intramolecular photocyclization of the anthracene chromophores occurs readily upon irradiation of dilute degassed solutions of all but **T1** acyclic receptors. In the case of **T1**, photoirradiation resulted in an uncharacterized mixture of products. This is presumably due to the small size of the spacer link between the receptor moiety and the anthracene groups, which hinders efficient [$4\pi + 4\pi$] cycloaddition. Although photodimerization of 9-substituted anthracenes can lead to the formation of head-to-head (HH) and head-to-tail (HT) photodimers, only HT products were isolated upon irradiation of **T3**−**T6**. A possible explanation is that both HT and HH cycloadducts are formed but that the latter are thermally labile and undergo retrocycloaddition during the course of the irradiation. It is well-known that head-to-tail (HT) photodimers are much more stable than their head-to-head (HH) counterparts[10] as evidenced by the ease in which they are generally isolated and characterized. By comparison, the corresponding HH dimers have much shorter half-lives due to additional steric and oxygen lone-pair repulsions that are absent in HT dimers.[10] Since no fast recovery of the anthracene chromophore was observed upon standing of the **T*n*** receptors following irradiation, it can be deduced that, if formed, HH dimers spontaneously revert to the starting material during the course of irradiation. With the exception of **T4**, the measured quantum yields for photodimerization in the absence of **6** are identical within experimental error (Table 3). The considerably higher propensity of **T4** toward photodimerization ($\Phi r = 0.15$) is accompanied by a reduction in fluorescence yield for this compound (in fact, $\Phi f + \Phi r$ is approximately constant for **T3**−**T6**). This suggests, albeit indirectly, that fluorescence emission from the locally excited state and photodimerization have as a common intermediate the same S_1 locally excited state and that photoreactivity is not solely controlled by the ground-state conformational population of the chromophores at the time of the excitation.

(23) Hamilton, A. D.; Van Engen, D. *J. Am. Chem. Soc.* **1987**, *109*, 5035.
(24) In the case of **T6C**, the addition of barbital also had a significant effect on the shift of other proton signals. In particular, the signals for the OCH_2 and the central photodimer CH protons moved downfield by +0.37 and +0.17 ppm, respectively.
(25) Hager, K.; Franz, A.; Hirsch, A. *Chem.—Eur. J.* **2006**, *12*, 2663.

Moreover, photoproduct **T4C** is unique among these receptors in having strong intramolecular H-bonds (Figure 2), which may contribute to form a pre-organized structure in the excited state promoting photodimerization.

As expected, photocyclization yields are strongly affected by the presence of **6**, which binds within the cavity of the receptor moiety located between the two anthracene chromophores. In the case of **T3**−**T5**, the net overall effect is to reduce the efficiency of dimerization from ca. 10 to 1−5%. This effect is particularly dramatic for **T4**, which undergoes a 3-fold reduction of its dimerization yield and is consistent with the loss of intramolecular H-bonding in the transition-state affecting photoreactivity. However, on a purely thermodynamical basis, the significantly greater binding affinity of **T*n*** versus **T*n*C** for **6** is expected to reduce the overall driving force for dimerization by providing greater stabilization for the acyclic forms as compared to the cyclized products. Assuming that the guest is at least partially released in the transition state toward cyclization, this would increase the activation energy for cyclization of the acyclic receptor in the presence of **6**. For **T6**, however, the situation is reversed, and the efficiency of cyclization is higher in the presence of **6** than in its absence. This result would be consistent with the larger receptor being able to maintain its H-bonded complex with **6** to a greater extent as photodimerization proceeds, thereby stabilizing the transition state. This observation is reminiscent of the templating effect of a barbituric acid analogue on the intermolecular dimerization of conjuguated alkenes possessing complementary H-bonding motifs.[9] In this system, however, the supramolecular control of the excited-state reactivity induced by the template is further modulated by the conformational control instilled by the polymethylene tether linking the anthracene chromophores to the H-bonding unit.[26] Finally, it is worth noting that the accrued photoreactivity of **T6** in the presence of barbital is accompanied by a decrease in the lifetime of the excimer as compared to **T5**, even though its fluorescence emission is very similar (Figure 6b, red and blue lines), suggesting similar excimer geometries. Taken together, these results are consistent with the emissive excimer located on the reaction pathway of the photocyclization reaction. However, it cannot be completely excluded that the formation of the fluorescent excimer observed in the LIF experiments is in competition with the formation of a reactive but nonemissive excimer leading to the photoproducts.

As commonly observed for anthracene cyclodimers, heating solutions of **T3**−**T6** in a nonpolar solvent such as toluene results in retrocyclization to the acyclic receptors. This, of course, offers the possibility of cycling a receptor between an acyclic form with high affinity and a closed form with low affinity. The degree of control that is obtained can be characterized by the ratio of the binding constants for the acyclic and cyclized forms toward a particular guest, which, as described previously, is found to decrease with increasing chain length for guests **6** and **7** (Figure 7). Cycling between the closed and the open forms of the receptors can be easily accomplished by heating the closed receptors **T*n*C** to obtain the open forms (**T*n***), which can be recyclized by irradiation. Repeated cycling was investigated using **T5** and **T5C** by monitoring the absorbance of the anthracene moiety (Figure 3). It can be noted that although the photocyclization reaction appears to be quantitative in each step, the thermal reopening induces slight (ca. 8%) degradation. The observed fatigue is thus a result of a small degree of degradation of the sample due to the necessity to heat the closed forms to relatively high temperatures for extended periods of time to return to the open forms.

Conclusion

The association of a H-bonding receptor site with an anthracene photoactive moiety is a viable approach to constructing photoactive receptors for neutral molecules. The systems are designed so that irradiation results in efficient [$4\pi + 4\pi$] photodimerization of the pendant anthracenes, which induces an important modification of the receptor binding site. These photoreceptors possess the capability of being photoinhibited, with binding constants that, in favorable cases, decrease by 3 orders of magnitude upon photocyclization. The photorelease of guests upon irradiation offers interesting perspectives for photoinduced control of molecular recognition events. The system can be recycled by heating the closed receptors to obtain the open forms, and future improvements could be oriented toward reducing fatigue in this step by facilitating the thermal retrodimerization of anthracene HT dimers. From the detailed examination of the ground- and excited-state behavior of the open and cyclized receptors as a function of tether size, the complex interplay between subtle counteracting forces emerges. The shorter tethers allow much greater discrimination to be obtained between the binding affinities of the open and the cyclized forms, whereas only the longest tether appears to facilitate photodimerization in the presence of barbital. The combination of these effects, conformational freedom of the polymethylene linker and the supramolecular control induced by the guest, must all be taken into account to adequately understand the properties and limitations of these photoregulated receptors.

Experimental Section

Spectroscopic and Photochemical Measurements. Fluorescence emission spectra were recorded on dilute (abs <0.2 at 366 nm) samples that were degassed by repeated freeze−pump−thaw cycles and sealed. Fluorescence quantum yields were determined by comparison with quinine sulfate in 1 N sulfuric acid ($\Phi f = 0.54$).[20] The fluorescence decay measurements were measured using a single-photon counting apparatus equipped with a hydrogen flash lamp and the data were deconvoluted using the Decan 1.0 program.[27] Photoreaction quantum yields were determined upon excitation at 360 nm using Aberchrome 540 as a chemical actinometer on an optical bench equipped with a 2000 W Hg−Xe lamp and a monochromator. Samples (5×10^{-5} M) were stirred during the irradiation, and the amount of converted material was monitored at 10 min intervals by UV−vis spectroscopy by measuring the disappearance of the ^{1}La band of the anthracene at 370 nm until 90% of the starting material was converted. Solutions were allowed to stand for 2 min before measurement of the UV−vis spectrum. The quantum yield was determined from the linear portion of the absorbance versus irradiation time graph corrected for the absorbance by the sample. The preparative photocyclization reactions were carried out by irradiating degassed solutions of the receptors in dichloromethane using a Hg lamp (400 W) and a Pb$(NO_3)_2$/KBr (7.0 g L^{-1}/540 g L^{-1}) solution filter with stirring over a period of 12 h. Fatigue studies were performed with degassed toluene solutions of **T*n*** ($c = 5 \times 10^{-6}$ M) that were first photocyclized by irradiation on an optical bench and then heated

(26) Castellan, A.; Desvergne, J.-P.; Bouas-Laurent, H. *Chem. Phys. Lett.* **1980**, *76*, 390.

(27) de Roek, T.; Boens, N.; Dockx. J. DECAN 1.0; Leuven, Belgium, 1991.

in the dark at 80 °C until no more increase in the absorption of the anthracene band was detected (8 h). The amount of converted material was determined every hour by UV−vis spectroscopy as stated previously.

Binding Constants. Fluorescence Method. The receptor **T*n*** (solution concentration between 2×10^{-6} and 8×10^{-6} M) was titrated with a solution of guest (typical concentration between 5×10^{-4} and 5×10^{-3} M) dissolved in the same receptor solution. The decrease in fluorescence emission between 380 and 580 nm was monitored as a function of guest concentration with an excitation wavelength of 360 nm.

UV−Vis Method. A similar protocol to that used for the fluorescence titrations was followed, monitoring the modifications of absorbance between 280 and 330 nm. In both cases, the binding constants were calculated using the Letagrop-spefo program.[17]

^{1}H NMR Method. The receptor (solution concentration between 5×10^{-4} and 6×10^{-3} M) in 0.4 mL of $CDCl_3$ was titrated with a stock solution of guest (typical concentration between 1×10^{-2} and 6×10^{-2} M) in the same receptor solution. The downfield shifts of the receptor amide NH was monitored as a function of guest concentration. Addition was continued through 9−20 equiv. The resultant titration curve was analyzed by using a nonlinear regression method with the WinEqNMR[18] computer program.

General Procedure for the Synthesis of Ethyl-9-anthryloxy-alkyloate (2*n*). Anthrone (3.0 g, 15 mmol), K_2CO_3 (2.35 g, 17 mmol), and acetone (dried over molecular sieves, 150 mL) were placed in a 250 mL round-bottomed flask equipped with a reflux condenser. After the addition of ethyl-*n*-bromoenoate (0.023 mol, 1.5 equiv), the mixture was heated under reflux for 24 h. The mixture was then allowed to cool to room temperature and filtered, and the solvent was removed under reduced pressure. The residue was then dissolved in 50 mL of CH_2Cl_2, washed with H_2O (3×20 mL), and dried over $MgSO_4$. After removal of the solvent, the crude product was purified by column chromatography (see Supporting Information for exact conditions).

General Procedure for the Synthesis of Carboxylic Derivatives (3*n*). Compound **2*n*** (10 mmol) was dissolved in 80 mL of ethanol in a round-bottomed flask equipped with a reflux condenser. After the addition of an aqueous solution of NaOH (25 mmol in 10 mL), the mixture was heated under reflux for 14 h and then allowed to cool to room temperature. The solvent was then removed under vacuum, giving a solid that was then dissolved in 250 mL of distilled water. Addition of 1 mL of concentrated hydrochloric acid under stirring led to the precipitation of the compounds that were collected by filtration and dried under vacuum at 60 °C for 14 h.

General Procedure for the Synthesis of Activated Ester Derivatives (4*n*). Compound **3*n*** (4 mmol) and *N*-hydroxysuccinimide (1.1 equiv) were dissolved in dry ethyl acetate (40 mL). A solution containing *N*,*N*′-dicyclohexylcarbodiimide (1.1 equiv) in ethyl acetate (20 mL) was then added under stirring, which was maintained for 48 h. The mixture was then filtered, and the filtrate was concentrated under reduced pressure. The solution thus obtained was allowed to stand at 0 °C for 4 h, which led to precipitation of the desired compound that was used without further purification.

General Procedure for the Synthesis of Diaminopyridine Derivatives (5*n*). A large excess of 1,5-diaminopyridine (0.03 mol, 10 equiv) was suspended in dry CH_2Cl_2 (60 mL) along with *N*,*N*′-diisopropylethylamine (1.5 equiv, 4.5 mmol). A solution of **4*n*** (3 mmol, 1 equiv) in CH_2Cl_2 (20 mL) was then added dropwise with stirring at 25 °C. The mixture was then brought to reflux, which was maintained for 5 days. The mixture was allowed to cool and then filtered. The filtrate was washed with water (3×100 mL), and the organic phase was collected and dried over $MgSO_4$, and the solvent was removed under reduced pressure. The crude product was then purified by column chromatography on silica (eluent: CH_2Cl_2/ethyl acetate 80:20).

General Procedure for the Synthesis of Acyclic Receptors T*n*, *n* = 1, 3, 4, 5, 6. 5-*t*-Butylisophthalic acid (68 mg, 304 μmol) was suspended in dry CH_2Cl_2 (30 mL) to which one drop of anhydrous DMF was added. A solution of oxalyl chloride (1 mL, 11.5 mmol) in dry CH_2Cl_2 (20 mL) was then added dropwise, and the resulting mixture was heated under reflux for 14 h. The solution thus obtained was cooled, and the volatile components were removed under reduced pressure to afford a brown oil that was dried at 60 °C under vacuum for 5 h, dissolved in dry THF (20 mL), and added dropwise to a solution of **5*n*** (670 μmol) and triethylamine (720 μmol) in dry THF (40 mL) with stirring. After 14 h of stirring at 25 °C, the mixture was filtered, and the solvent was removed under vacuum. The solid thus obtained was purified by column chromatography on alumina (CH_2Cl_2/methanol, gradient 0−2%).

General Procedure for the Synthesis of Macrocyclic Compounds T*n*C, *n* = 3, 4, 5, 6. A solution of **T*n*** in 50 mL of distilled CH_2Cl_2 at $c = 5\ 10^{-4}$ M was degassed and irradiated under stirring for 14 h with a Hg Lamp. After removal of the solvent, the solid was dissolved in THF, precipitated with hexane, and dried at 25 °C under vacuum.

Acknowledgment. Financial support from the CNRS, the French ministry of Education and Research, the Région Aquitaine, and the EPSRC (award of PDRA Grant GR/S07438/02 to Y.M.) is gratefully acknowledged. We thank the EPSRC national mass spectrometry service (Swansea) for carrying out measurements.

Supporting Information Available: General experimental details, spectral characterization (^{1}H NMR, ^{13}C NMR, HRMS) for all compounds, and elemental analysis of **2*n***, **3*n***, and **T*n***. Job plot (**T5** with **6**) and NMR titration of **T3**, **T3C**, **T6**, and **T6C** with **6** and **T6** with **7**. This material is available free of charge via the Internet at http://pubs.acs.org.

JO061528A